

Photopyroelectric Detection of Phase Transitions in Solids

A. Mandelis, F. Care, and K. K. Chan

Photoacoustics Laboratory, Department of Mechanical Engineering,
University of Toronto, Toronto, Ontario, Canada, M5S 1A4

L. C. M. Miranda*

Center for Chemical Physics, University of Western Ontario, London, Ontario,
Canada N6A 3K7

Received 21 May 1985/Accepted 10 June 1985

Abstract. The recently developed photopyroelectric spectroscopy (P²ES) has been used to investigate phase transitions in solids. In our variable temperature experiments, specific heat curves for Rochelle Salt and V₂O₄ powders were obtained and found in good agreement with results obtained previously via more experimentally involved methods.

PACS: 64, 78

In the last few years, Photoacoustic Spectroscopy (PAS) [1–9] has been applied to the study of structural phase transitions in solids. In those studies both microphone-gas systems [1–6,8], and piezoelectric detection systems [7,9] to a lesser extent, were used together with solid materials exhibiting first- and second-order phase transitions. PAS was thus proven to be a technique sensitive to both kinds of phase transitions, giving mostly qualitative information concerning the temperature of the transition through both amplitude and phase channels. Siqueira et al. [3] and Fernández et al. [6] have pointed out that microphone-gas coupled PAS can yield quantitative information about the *product* of the temperature dependent thermal conductivity and the temperature dependent specific heat of a solid sample using the Rosencwaig-Gersho (RG) theory [10], provided the sample cell thermal response is known and normalized out in the entire temperature range of the experiment. Previously, Pichon et al. [2] used the RG theory to show that only in the special case of thermally thick solids does the photoacoustic signal solely depend on the specific heat and is independent of the thermal conductivity of the sample. Their theoretical predic-

tion was further shown to be in reasonable agreement with experimental photoacoustic data on single crystalline CrCl₃ between 15 and 10 K and on MnF around 68 K. From the work of these authors it is apparent that microphone-gas coupled PAS can be used to study specific heat transitions only in transparent and semi-transparent materials, due to the thermally thick requirement. Opaque materials could also be investigated, in principle, provided appropriately high beam modulation frequencies are used. In practice gas coupled PAS at those high frequencies (typically kHz and MHz range) is virtually impossible due to very poor signal-to-noise ratios (SNR) and microphone frequency response limitations.

Etxebarria et al. [7,9] have shown theoretically, using the Jackson and Amer's theory [11], and experimentally, that the piezoelectric photoacoustic signal is a function of sample specific heat only, and independent of thermal conductivity, in the optically and thermally thick limits. This observation is indicative of further restrictions on the opacity of the sample, in addition to the high modulation frequency requirements similar to the gas-coupled PAS.

In this work we present the first application of Photopyroelectric Spectroscopy (P²ES) [12–14] to the study of temperature-dependent phase transitions in solids. In particular, we demonstrate the usefulness of

* On leave of absence from the Instituto de Estudos Avancados, Centro Tecnico Aeroespacial, 12200 S.J. Campos, SP, Brazil

this technique to specific heat-data acquisition around the transition temperature for powdered samples exhibiting first- and second-order transitions. Both theoretical and experimental results indicate the capability of P²ES to measure specific heat profiles, using very simple experimental apparatus compared to other methods, while relaxing the often-too-stringent requirement of thermally thick and either transparent or opaque solids.

1. Theoretical

We assume a one-dimensional system geometry [14] and an optically opaque pyroelectric transducer. This assumption is well founded for the KynarTM polyvinylidene difluoride (PVDF or PVF₂) thin transducer films coated with nickel and exposed to He-Ne laser light at 632.8 nm in our experiments [15]. Taking into account the fact that the samples used in this work were optically opaque powders, the photopyroelectric theory [14] predicts the following expression for the pyroelectric voltage:

$$V(\omega_0) \cong 2A \left(\frac{\beta_s \eta_s}{k_s(\beta_s^2 - \sigma_s^2)\sigma_p} \right) (b_{sg} r_s + 1) / [(b_{sg} + 1)(b_{ps} + 1) \cdot \exp(\sigma_s L_s) + (b_{sg} - 1)(b_{ps} - 1) \exp(-\sigma_s L_s)], \quad (1)$$

where

$$A \equiv p I_0 / 2K \varepsilon_0, \quad (2)$$

$$b_{ij} \equiv k_i \sigma_i / k_j \sigma_j, \quad (3)$$

$$r_s \equiv \beta_s / \sigma_s; \quad (4)$$

p is the pyroelectric coefficient of the detector, I_0 is the intensity of the incident radiation on the sample, K is the dielectric constant of the detector and ε_0 the permittivity constant of vacuum; k_i is the thermal conductivity of the i^{th} material and σ_i is the material's complex thermal diffusion coefficient [10]; β_s, η_s, L_s are the sample optical absorption coefficient, non-radiative quantum efficiency and thickness, respectively. For photopyroelectric cells with solid-air coupling $b_{sg} \gg 1$ and for opaque samples $|r_s| \gg 1$ [10]. Using PVF₂ parameters [16] and assuming crystalline silicon:

$$b_{ps} = k_p \sigma_p / k_s \sigma_s = k_p \alpha_s^{1/2} / k_s \alpha_p^{1/2} = 9.6 \times 10^{-2} \ll 1,$$

where α_i is the thermal diffusivity of material (i). It ought to be mentioned that (1) is strictly valid in the limit of thermally thick pyroelectric film [14]. This condition is satisfied when

$$f_0 \gg \alpha_p / \pi L_p^2, \quad (5)$$

where f_0 is the light intensity modulation frequency, L_p is the pyroelectric film thickness ($= 28 \mu\text{m}$), and $\alpha_p = 5.4 \times 10^{-8} \text{ m}^2/\text{s}$. Inequality (5) shows that an experiment is well within the transducer thermally thick region for chopping frequencies $f_0 \gg 20 \text{ Hz}$. In the transducer thermally thin limit the theory [14] produces an expression similar to (1) with L_p replacing $1/\sigma_p$ inside the first set of brackets.

Equation (1) simplifies considerably for optically opaque solids

$$V(\omega_0) = A(\eta_s/\sigma_p) [k_s \sigma_s \sinh(\sigma_s L_s)]^{-1}. \quad (6)$$

If the solid is thermally thin, such as is the case at low frequencies, expansion of the sinh in (6) and retention of the first term only yields

$$V[(\omega_0; C_s(T))] = \frac{B}{\omega_0^{2/3} C_s(T)}; \quad B \equiv \text{const} \quad (7)$$

for frequencies such that the transducer is thermally thick; and

$$V[\omega_0; C_s(T)] = \frac{B'}{\omega_0 C_s(T)}; \quad B' \equiv \text{const} \quad (8)$$

for frequencies such that the transducer is thermally thin. Equations (7 and 8) show the advantage of P²ES over PAS as a method for the *direct* measurement of the specific heat of the thermally thin sample, $C_s(T)$, at low frequencies where large SNRs are expected. Equations (7, 8) are to be compared to the PAS signal [3]

$$Q[\omega_0; T] = \frac{B''(\omega_0)}{[C_s(T)k_s(T)]^{1/2}} \quad (9)$$

for thermally thick samples, at high frequencies.

Equations (7, 8) must be multiplied by a temperature dependent function $f(T)$, accounting for the thermal response of the P²ES cell, which must be determined experimentally [3]. Therefore, in general

$$V[\omega_0; C_s(T)] = \text{const}(\omega_0) [f(T)/C_s(T)].$$

To determine $f(T)$ the P²ES response of a sample with known thermal behavior is required. In our experiments we used a (100) silicon wafer, n -type, as the reference. The normalized value for $f(T)$ can be calculated then from the photopyroelectric signal V_{Si} ; and from the relation:

$$\overline{f(T)} \equiv \frac{f(T)}{f(T_{\text{ref}})} = \left(\frac{V_{\text{Si}}(\omega_0; T)}{V_{\text{Si}}(\omega_0; T_{\text{ref}})} \right) \left(\frac{C_{\text{Si}}(T)}{C_{\text{Si}}(T_{\text{ref}})} \right) \quad (10)$$

using the values of $C_{\text{Si}}(T)$ available in the literature [17, 18]. T_{ref} was chosen to be the room (laboratory) temperature throughout the duration of our experiments. Equation (10) can be written in the normalized form

$$\overline{f(T)} = \overline{V_{\text{Si}}(T)} \cdot \overline{C_{\text{Si}}(T)}. \quad (11)$$

When a material specimen is substituted for the reference silicon crystal, (11) becomes

$$\overline{f(T)} = \overline{V_s(T)} \cdot \overline{C_s(T)}. \quad (12)$$

Now, (11, 12) can be solved for the quantity of interest, $\overline{C_s(T)}$:

$$\overline{C_s(T)} = \overline{f(T)} / \overline{V_s(T)} = [\overline{V_{Si}(T)} / \overline{V_s(T)}] \overline{C_{Si}(T)}. \quad (13)$$

All the quantities on the right-hand side of (13) can either be measured photopyroelectrically, or have known literature values. Equation (13) is to be compared to its photoacoustic counterparts [3, 6]:

$$\overline{C_s(T)} \cdot k_s(T) = [F(T) / Q_s(T)]^2 \quad (14)$$

where $F(T)$ is a temperature dependent function of the thermal response of a gas-coupled PAS cell, and $Q_s(T)$ is the photoacoustic signal.

2. Experimental

The materials chosen to demonstrate the ability of P²ES to monitor structural phase transitions in solids were powders of 0.6 at.-% Al-doped vanadium oxide, V₂O₄:Al, and Rochelle Salt, NaKC₄H₄O₆ · 4H₂O. These materials were selected because they exhibit first-order [19] and second-order [20] phase transitions, respectively, in the temperature range between 270–350 K, which was most convenient to implement into our experimental apparatus.

The experimental system used for our experiments was essentially the same as the one described previously [13]. The main difference here was the use of an aluminum P²ES cell, instead of teflon, for improved electromagnetic shielding of the pyroelectric circuit as required for optimal SNRs, and rapid absorption and distribution of heat throughout the cell mass as needed for the steady-state temperature dependent experiments. The aluminum cell was further supplied with a YSI 44108 Precision teflon covered thermistor in order to measure the sample compartment temperature approximately 5 mm above the 28 μm thick PVF₂

pyroelectric film transducer/sample holder. The sample compartment was isolated from environmental temperature fluctuations with a screw-on plexiglas cover, which was transparent to the Uniphase 1101 lmW He–Ne laser acting as the exciting light source. The cell was heated up to a pre-determined temperature after calibration, in a non-contact fashion using radiant heat from a CGE red bowl-hardglass brooder lamp. The intensity of the radiation was controlled via a Superior Electric Co. 117T Powerstat Variac.

In order to achieve the expected low temperatures required for a phase transition in Rochelle Salt from monoclinic to rhombic ($T_c = 296$ K [20]) below the ambient temperature, the cell was placed in an ice bath and was slowly heated by the brooder lamp until the desired temperature was reached. The cell exhibited transient heating upon shining the lamp for ca. 1 h until steady state was achieved, with shorter transients at high temperatures, as shown in Fig. 1.

The (100)Si reference crystal used in this work was placed in the sample chamber on carefully flattened PVF₂ film to maximize the direct contact area. Furthermore, to evaluate the importance of air gaps between sample and transducer, another experiment was performed with the same wafer and a thermal compound thin film interface between sample and transducer to reduce the interfacial thermal resistance. Frequency-dependent P²ES signals obtained from these two experiments showed substantial enhancement from the sample with the thermal compound and an essentially rigid shift of the signal with no change in the frequency response, as shown in Fig. 2. Therefore, no evidence of signal distortion from interfacial thermal resistances was found and the rest of our experiments were performed without the thermal compound, as satisfactory SNRs could be easily achieved at low light modulation frequencies. Figure 3 shows the P²ES amplitude as a function of chopping period, $1/f_0$, for Si. The curve exhibits a change in slope and a “knee” at approximately $125 \text{ Hz} \leq f_0 \leq 240 \text{ Hz}$. This frequency range is consistent with the calculated

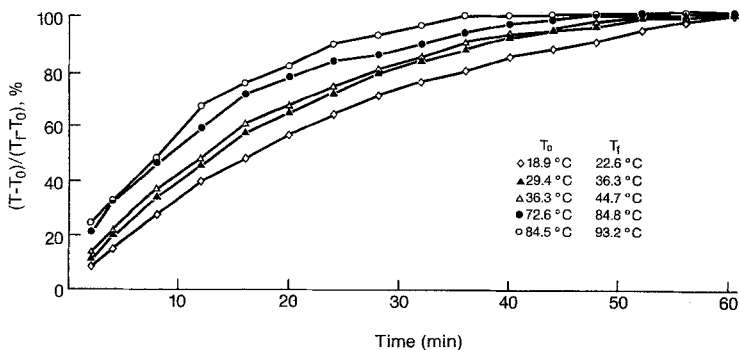


Fig. 1. Temporal response to temperature step inputs of aluminum P²ES cell. (T_0 : initial temperature; T_f : final temperature)

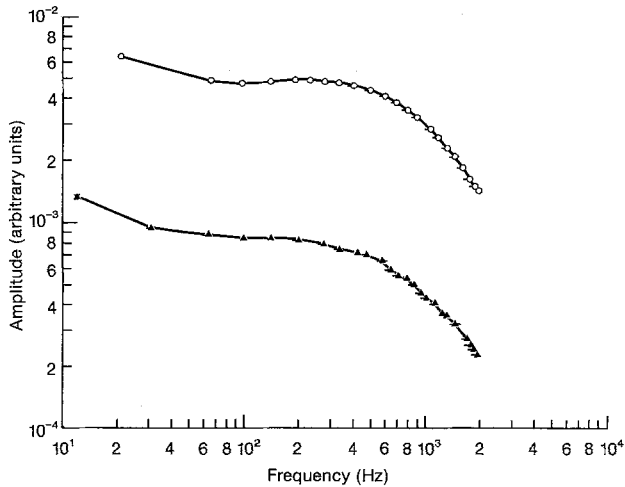


Fig. 2. Photopyroelectric amplitude frequency response of (100) n-type Si wafer. ○ = With thermal compound interface between sample and PVF₂ film; ▲ = Without thermal compound interface

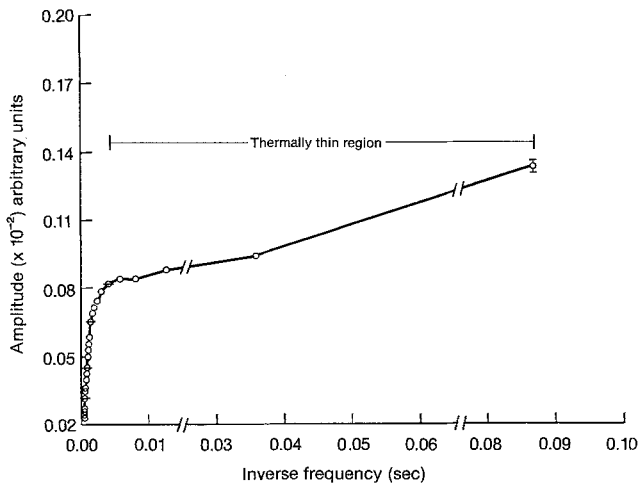


Fig. 3. Photopyroelectric amplitude vs. f_0^{-1} for (100) n-type Si wafer. He-Ne laser illumination

sample transition frequency from thermally thin to thermally thick at ca. 150 Hz ($\alpha_{Si} = 1.06 \text{ cm}^2 \text{ s}^{-1}$, $L_{Si} = 480 \mu\text{m}$).

Figure 4 shows the measured thermal factor, $\overline{f(T)}$, of the cell using (11), with $\overline{C_{Si}(T)}$ calculated from [17, 18]

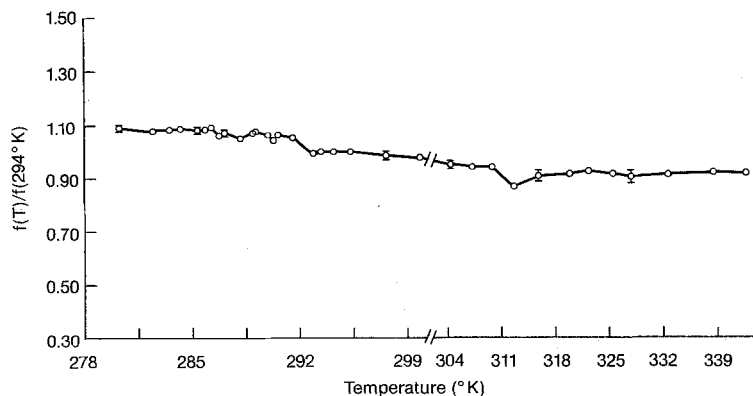


Fig. 4. P²ES cell temperature normalized characteristic factor $\overline{f(T)}$ under He-Ne laser illumination ($f = 32 \text{ Hz}$)

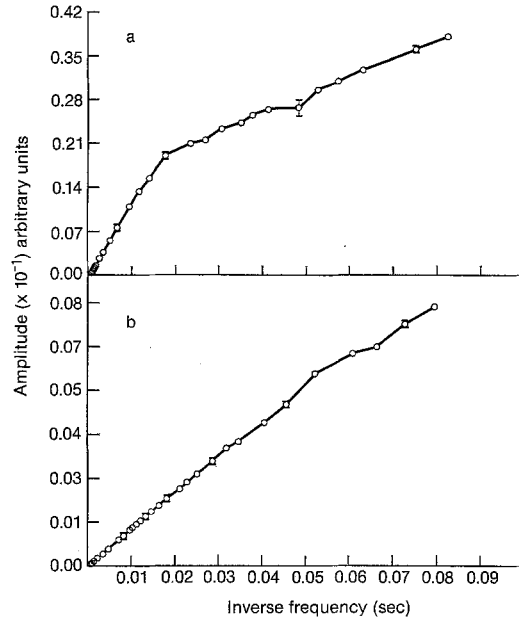


Fig. 5. (a) Photopyroelectric amplitude vs. f_0^{-1} for 0.6 at.-% Al-doped V₂O₄ at 632.8 nm excitation. The “knee” occurs at ca. 35 Hz. (b) Same plot for Rochelle Salt

and $\overline{V_{Si}(T)}$ being the amplitude of the P²ES signal at $f_0 = 32 \text{ Hz}$. At this frequency, condition (5) and Fig. 3 show that both sample and PVF₂ detector are thermally thin, silicon also being optically opaque. The fulfilment of these conditions does validate (11) on which the accurate determination of $\overline{f(T)}$ depends.

Figure 5 shows the P²ES vs. chopping period behavior of V₂O₄:Al (Fig. 5a), and Rochelle Salt (Fig. 5b). Within the frequency span of the experiment (10 Hz–1 kHz) the signal amplitude from V₂O₄:Al exhibits two regions: the low frequency region ($f_0 \lesssim 30 \text{ Hz}$) with $V(\omega_0) \propto \omega_0^{-1 \pm 0.1}$, and the high frequency region ($f_0 > 35 \text{ Hz}$) where $V(\omega_0) \propto \omega_0^{-1.5 \pm 0.2}$. The “knee” could not, unfortunately, be directly related to sample thickness, because the latter was a thin layer of V₂O₄:Al powder with variable thickness from site to site. The frequency response of the powdered thin layer of Rochelle Salt, however, showed no “knee”, with

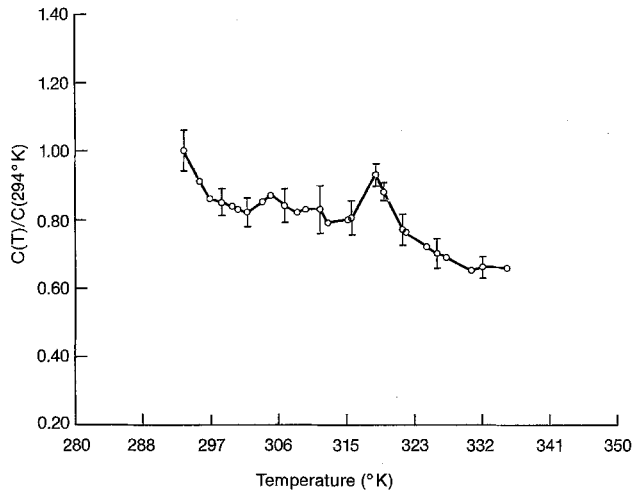


Fig. 6. Normalized P²ES signal amplitude vs. T for 0.6 at.-% Al-doped V_2O_4 powders; $f_0 = 12$ Hz. $T_c = 319 \pm 1$ K

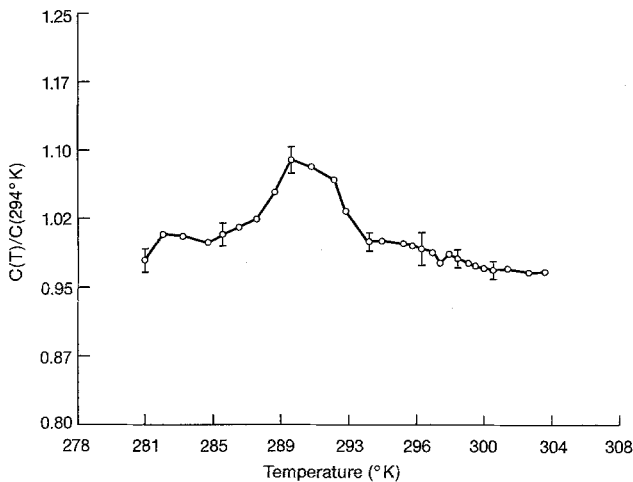


Fig. 7. Normalized P²ES signal amplitude vs. T for ferroelectric $NaKC_4H_4O_6 \cdot H_2O$ (Rochelle Salt); $f_0 = 12$ Hz. $T_c = 291 \pm 2$ K

$V(\omega_0) \propto \omega_0^{-1 \pm 0.05}$ (Fig. 5b). It was concluded, therefore, that both samples were thermally thin below ca. 35 Hz, and, in accordance with the theory [14], the PVF₂ transducer was also thermally thin. A constant chopping frequency of 12 Hz was subsequently used to monitor the P²ES signal through the phase transition temperatures. The use of this and vicinal frequencies validates (13) and renders P²ES to a specific heat measuring method.

Figure 6 is a plot of $f(T)/V_s(T)$ vs. T for $V_2O_4:Al$. According to (13) this plot should be directly related to the specific heat of this material normalized by its value at 294 K. Data from Fig. 4 were used in the calculation of $f(T)$. Figure 6 shows a rather narrow but well-characterized peak centered at ca. 319 ± 1 K, with a FWHM of ca. 4 K.

Figure 7 is a similar plot for Rochelle Salt. The peak is centered at ca. 291 ± 2 K with a FWHM of 4.5 K.

3. Discussion

Pure V_2O_4 has been known to crystallize in a tetragonal structure above a transition temperature T_c of ca. 340 K [19]. This is a first-order transition with a discontinuity in the value of the specific heat involving a latent heat estimated at 1020 ± 5 cal/mole of V_2O_4 . Above T_c the material behaves as a metal with a tetragonal structure with nearly regular oxygen octahedra sharing edges along the c -axis. At temperatures below T_c , the structure becomes monoclinic as vanadium pairing occurs along the pseudorutile c -axis [21]. In this temperature region V_2O_4 behaves electrically as a semiconductor. When V_2O_4 is doped with Al, the T_c decreases nonlinearly with increasing atomic percent of aluminum. According to phase diagrams by Reyes et al. [21], T_c for our 0.6 at.-% Al-doped V_2O_4 is 322 K, in very good agreement with the position of the photopyroelectric peak of Fig. 6. Siqueira et al. [3], using an experimentally much more involved temperature-controlled photoacoustic apparatus than our simple set-up, have plotted the PAS signal vs. temperature for a 0.8 at.-% Al-doped VO_2 sample. According to (14) this signal was proportional to the product of the specific heat and the thermal conductivity of the sample through the phase transition temperature, 320 K [3, 21]. The experimental results of these authors show a change in the slope of the otherwise monotonically increasing $\overline{C_s(T)} \cdot \overline{K_s(T)}$ vs. T curve at that temperature. We believe that the existence of a sharp transition peak in the P²ES spectrum of Fig. 6 can locate T_c more accurately than the slope change in the data of Siqueira et al. [3].

The Rochelle Salt is a ferroelectric material undergoing a spontaneous polarization transition of the second order, which does not involve a latent heat but a discontinuity in the specific heat only [20]. The structure of this salt changes from monoclinic to rhombic above the transition temperature of 296 K [22]. There has been a further transition observed from monoclinic to rhombic below 255 K [22]. In the temperature range of our experiments, Fig. 7, the observed transition temperature $T_c = 291 \pm 2$ K is somewhat lower than Halblützel's early work. The discrepancy could be traced in many factors, such as the fact that in his work the T_c was determined from plots of the logarithm of the dielectric constant of the material vs. T . Further, the powdered nature of our samples and the positioning of the thermistor ca. 5 mm above the sample surface may be easily responsible for temperature discrepancies of up to 5 K. Lastly, the accuracy of temperature measuring ap-

paratus in those studies done approx. half a century ago, such as is the case with Halblützel's work, may very well be suspect.

4. Conclusions

In this paper we have described the first applications of P²ES to structural phase transitions of first and second-order in powdered solids. The principal merits of the technique appear to be a) the simplicity of the experimental apparatus compared to temperature-dependent measurements using PAS; and b) the dependence of the thermally thin P²ES signal directly on $C_s(T)$. This feature is a distinct advantage over PAS and renders this technique to a direct method of measuring specific heat of solids which may be difficult or impossible to measure otherwise, such as opaque powders, polycrystalline solids etc. The main limitation of our method appears to be the rather restrictive temperature range within which PVF₂ can be safely used without being damaged: maximum operating temperature is 80–120 °C; minimum recommended temperature is –40 °C [16]. Other pyroelectrics may be used, of course, if an increased temperature span response is required.

Acknowledgements. The authors wish to acknowledge the support of the National Science and Engineering Research Council of Canada during this work. One of us (L.C.M.M) wishes to thank the Canadian and Brazilian Research Councils for their support during his visiting period at the University of Western Ontario.

References

1. R. Florian, J. Pelzl, M. Rosenberg, H. Vargas, R. Wernhardt: *Phys. Stat. Solidi A* **48**, K35 (1978)
2. C. Pichon, M. Le Liboux, D. Fournier, A.C. Boccara: *Appl. Phys. Lett.* **35**, 435 (1979)
3. M.A.A. Siqueira, C.C. Ghizoni, J.I. Vargas, E.A. Menezes, H. Vargas, L. C. M. Miranda: *J. Appl. Phys.* **51**, 1403 (1980)
4. P. Korpiun, J. Baumann, E. Lüscher, E. Papamokos, R. Tilgner: *Phys. Stat. Solidi A* **58**, K13 (1980)
5. P.S. Bechthold, M. Campagna, T. Schober: *Solid State Commun.* **36**, 225 (1980)
6. J. Fernández, J. Etxebarria, M.J. Tello, A. López Echarri: *J. Phys. D* **16**, 269 (1983)
7. J. Etxebarria, S. Uriarte, J. Fernández, M.J. Tello, A. Gómez-Cuevas: *J. Phys. C* **17**, 6601 (1984)
8. I. Bibi, T.E. Jenkins: *J. Phys. C* **16**, L 57 (1983)
9. J. Etxebarria, J. Fernández, M.A. Arriandiaga, M.J. Tello: *J. Phys. C* **18**, L 13 (1985)
10. A. Rosencwaig, A. Gersho: *J. Appl. Phys.* **47**, 64 (1976)
11. W. Jackson, N.M. Amer: *J. Appl. Phys.* **51**, 3343 (1980)
12. H. Coufal: *Appl. Phys. Lett.* **44**, 59 (1984)
13. A. Mandelis: *Chem. Phys. Lett.* **108**, 388 (1984)
14. A. Mandelis, M. Zver: *J. Appl. Phys.* **57**, 4421 (1985)
15. W.R. Belvin, J. Geist: *Appl. Opt.* **13**, 1171 (1973)
16. Kynar™ Piezo Film Technical Manual (1983), Pennwalt Corp. 900 First Ave., King of Prussia, PA, p. 17
17. Y.S. Touloukian: *Thermophysical Properties of High Temperature Solid Materials*; Vol. 1 (Thermophysical Properties Res. Ctr., Purdue Univ.) p. 886
18. C. Kittel: *Introduction to Solid State Physics*, 5th edn. (Wiley, New York 1976) p. 128
19. W. Paul: *Mater. Res. Bull.* **5**, 691 (1970)
20. A.J. Dekker: *Solid State Physics* (Prentice-Hall, Englewood Cliffs, NJ 1954) p. 202
21. J.M. Reyes, S.L. Segel, M. Sayer: *Can. J. Phys.* **54**, 1 (1976)
22. J. Halblützel: *Helv. Phys. Acta* **12**, 489 (1939)